LETTER

Fabrication of 3D Copper Oxide Structure by Holographic Lithography for Photoelectrochemical Electrodes

Woo-Min Jin, Ji-Hwan Kang, and Jun Hyuk Moon*

Department of Chemical and Biomolecular Engineering, Sogang University, 1 Sinsu-dong Mapo-gu, Seoul, 121-742, South Korea

ABSTRACT We fabricated three-dimensional copper oxide structure by holographic lithography and electroless deposition. A five-beam interference pattern defined a woodpile structure of SU-8. The surface modification of SU-8 structure was achieved by multilayer coating of polyelectrolyte, which is critical for activating the surface for the reduction of copper. Copper was deposited onto the surface of the structure by electroless deposition, and subsequent calcinations removed the SU-8 structure and simultaneously oxidized the copper into copper oxide. The porous copper oxide structure was used as a photoelectrochemical electrode. Because of the highly porous structure, our structure showed higher photocurrent efficiency.

KEYWORDS: holographic lithography • electroless deposition • surface modification of SU-8 • photoelectrochemical electrode

INTRODUCTION

Copper oxide in the form of cuprous oxide (Cu_2O) or cupric oxide (CuO) is a p-type semiconducting material with a relatively low direct bandgap of ~2 or ~1.2 eV, respectively, which makes it a suitable candidate for photonic and photoelectrochemical applications such as photonic crystals, solar cells, and photocatalysts (1−5).For example, copper oxide has been used as a visible-light catalyst in the production of hydrogen to be used as an alternative energy source, and in the degradation of organic molecules for environment (4). Meanwhile, for photoelectrochemical applications, porous copper oxide structures have been attracted because porous structures can provide larger surface areas, thus enabling higher electrochemical reaction rates as well as greater absorption of light. Previously, copper oxide was grown under an electric field and electrodeposited with a surfactant to produce mesostructured copper oxide particles and their assembled films (6, 7). However, in these approaches, the control of pore size or organization are not allowed. Instead, templating methods, such as the use of sacrificial colloidal crystals of monodispersed particles have been recently applied to produce porous copper oxide particles (1, 8). In a typical procedure using a template, a polymeric colloidal particle assembly was formed. The deposition of copper and subsequent removal of colloidal particles by heat treatment generated copper oxide porous films. A major advantage of the colloidal crystal template method is the ability to control the pore size easily by varying the size of the particles.

In this communication, we report the application of three-dimensional (3D) holographic lithography and electroless deposition to produce porous copper oxide structures for use as photoelectrochemical electrodes. Compared with using colloidal crystal templates, holographic lithography is a more flexible approach as it permits access to a variety of morphologies, including various lattice symmetries and volume fractions, through appropriate arrangements of the laser beams and exposure conditions (9). Meanwhile, previously, 3D holographic lithography templates and electrodeposition have been used to produce 3D copper oxide photonic crystals (1). Here an electroless deposition method was successfully applied for the deposition of copper oxide into holographic lithography templates. For this purpose, we introduce a facile modification method of SU-8 photoresists by layer-by-layer coating of polyelectrolytes to activate SU-8 surface and apply a conformal shell of copper by electroless deposition. Photoelectrochemical reactions using the lithographically defined copper oxide structure were investigated. The photoelectrochemical responses under visible light were compared with the performance using a flat copper oxide film. 3D woodpile porous copper oxide electrodes show a three times increase of the cathode photocurrent when exposed to light.

EXPERIMENTAL METHODS

Preparation of a 3D Woodpile Structure. A 3D woodpile structure was obtained via multibeam holographic lithography. The photoresist was prepared by mixing epoxy-based resin (EPON SU-8, Miller-Stephenson Chemical) and a photoinitiator (Irgacure 261, Ciba, 2 wt %) in a solvent (gamma-butyrolactone (GBL), Sigma-Aldrich). A photoresist film with a thickness of 4−6 μm was obtained by spin-casting on a fluorine-doped tin oxide (FTO) glass substrate. The film was soft-baked at 95 °C for 10 min before being exposed to the interference pattern. The diameter of the laser beam used for the interference pattern (Ar-ion laser, wavelength 488 nm, coherent) was expanded by a factor of

* Corresponding author. E-mail: junhyuk@sogang.ac.kr.
Received for review August 21, 2010 and accepted October 29, 2010
DOI: 10.1021/am100773h

Published on Web 11/09/2010

Scheme 1. Fabrication of the 3D Woodpile Copper Oxide Structures: (a) SU-8 Surface Activation by Formation of Pd Catalysts with the Assistance of Layer-by-Layer Coating of Polyelectrolytes. (b) Electroless Deposition of Copper and Subsequent Calcinations for 3D Copper Oxide Structures

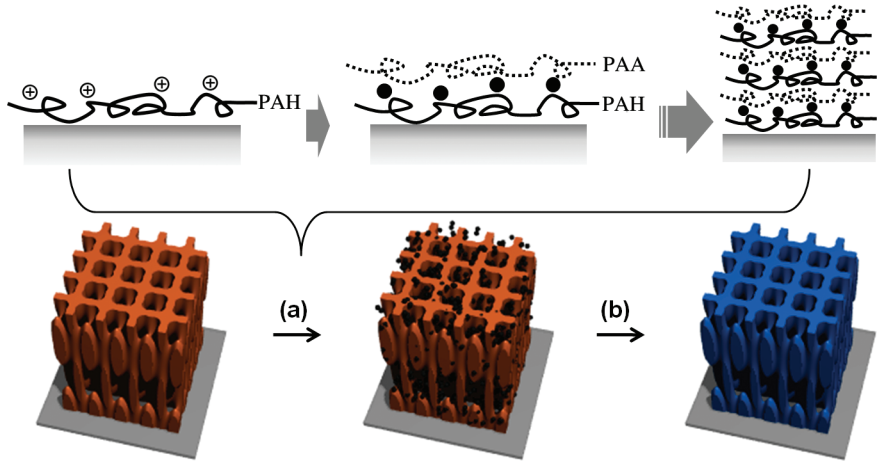

3 using a Galilean beam expander (Thorlabs). The laser beam was incident on the photoresist through a top-cut four-sided fused silica prism, which had a refractive index of 1.48 at a wavelength of 488 nm and was positioned with the surface perpendicular to the laser beam. The photoresist was exposed to the beam for 0.5 s to create the interference pattern. After postexposure baking at 95 °C, the sample was developed with PGMEA (propylene glycol methyl ether acetate, Sigma-Aldrich) and rinsed with 2-propanol.

Activation of the SU-8 Surface. The surface of the SU-8 pattern was activated by coating with a palladium (Pd) catalyst; alternating coatings of polyelectrolyte and Pd catalyst solution were applied to the SU-8. For polyelectrolytes, poly(allylamine hydrochloride) (PAH) (M_w 70 000, Aldrich) and poly(allylamine hydrochloride) (PAA) (M_w 90 000, Aldrich) solutions were dissolved in deionized water and the pH was controlled for both solutions at 7.5 and 3.5, respectively, using 1 M NaOH for pH 7.5 and 1 M HCl for pH 3.5. The catalyst solution was prepared by dissolving Na_2PdCl_4 in HCl solution (pH 2.5). The SU-8 pattern was dipped in PAH solution, Pd catalytic solution, and then PAA solution. This process was repeated and the substrate was washed thoroughly with distilled water in between each step.

Copper Electroless Deposition. The copper electroless deposition bath was prepared by mixing 0.04 M copper sulfate (Aldrich), ethylenediaminetetraacetic acid (EDTA, Aldrich), 50 ppm 2,2′-dipyridyl (Aldrich), and 0.05 M formaldehyde solution (Aldrich) in deionized water. The pH of the solution was controlled to be 12−13 by adding NaOH solution (50%). The deposition of copper was achieved by dipping the activated SU-8 templates in the prepared copper electroless deposition solution at 70 °C.

Photoelectrochemical Measurement. Photoelectrochemical studies of copper oxide were performed by applying the copper oxide film as a working electrode. Photocurrent characterization was performed using a potentiostat (Versastat, AMETEK); the scan ranged from 0.0 V to −0.4 V at a rate of 0.1 V/s under visible laser light exposure (Ar-ion laser, wavelength 488 nm). A platinum wire and a saturated calomel electrode were used as the counter and reference electrodes, respectively. An aqueous electrolyte solution of 0.5 M Na_2SO_4 was prepared and oxygen was bubbled through it for 30 min before the measurement.

Characterization. The copper oxide microstructure was measured by SEM (Hitachi). The film composition of the catalyst activated SU-8 surface was evaluated using an energy-dispersive spectroscopy (EDS) device attached to the SEM. The crystal structure and orientation of the copper oxide film were investigated by X-ray diffraction (XRD) with Cu Kα radiation.

RESULTS AND DISCUSSION

The fabrication procedure for the copper oxide woodpile electrodes is shown in Scheme 1. The woodpile structure was created by a five-beam interference pattern using a multifaceted prism. The surface of the SU-8 was treated with polyelectrolyte multilayers to adsorb catalyst ions. This was followed by electroless deposition to apply a copper coating to the woodpile structure. The SU-8 templates were removed by heat treatment, and simultaneously, the copper was oxidized to copper oxide, leaving behind 3D woodpile copper oxide structures.

The beams of the five-beam interference pattern produced by the prism possess wave-vectors of k (0, 0, 1), k ($-\sin\theta$, 0, $\cos\theta$), k (0, $-\sin\theta$, $\cos\theta$), k ($\sin\theta$, 0, $\cos\theta$), and k (0, $\sin\theta$, $\cos\theta$), where $k = 2\pi/\lambda$, λ is the wavelength of the laser beam (488 nm) and θ is the angle between the side beams and the central beam (30°) (10). The polarizations of the five beams as follows: the unit polarization of the central beam was ±(0.71, 0.71, 0) and the unit polarizations of the side beams were ±(0.59, 0.60, −0.35), ±(0.59, 0.60, 0.35), ±(0.60, 0.59, −0.35), and ±(0.60, 0.59, 0.35).

The iso-intensity surface of the interference pattern of these beams is shown in the inset image of Figure 1a. The ratio between lattice distance on the surface and the layer-by-layer distance in the vertical direction of the film was to be 1:2.5. Figure 1a,b shows SEM images of the holographic woodpile structure of SU-8 fabricated by exposure to five-

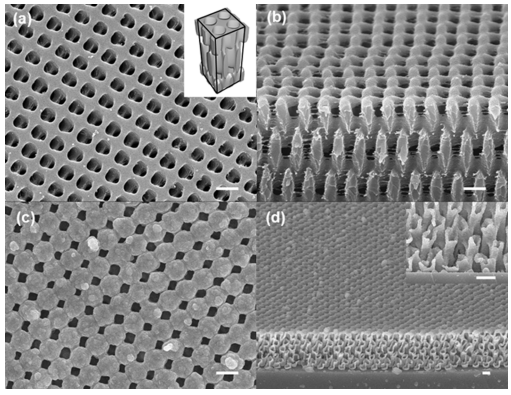

FIGURE 1. SEM images of SU-8 woodpile structures fabricated by holographic lithography and their inverted copper oxide structures. (a) Surface image of SU-8 woodpile structures and (b) their cross-sectional image. The inset shows a simulated surface of woodpile interference patterns. (c) Surface image of copper oxide and (d) their cross-sectional image. The inset shows the magnified image of the cross-section of copper oxide. (Scale bar, 1 μm.)

Table 1. EDX Analysis of SU-8 Surface Treated by Catalyst Solution without and with Layer-by-Layer Coating of Polyelectrolytes

sample	C %	O %	Pd %
bare SU-8	77.26	22.74	0.00
polyelectrolyte-treated SU-8	77.81	16.49	6.70

beam interference. Previously, it has been reported that the phase of the one beam in a five-beam interfering beam determines whether the symmetry of the woodpile structure is diamond or FCC (11). In our experiment, we obtained woodpile structures of the type shown in Figure 1, that is, with the *x*- and *y*-rods stacked alternately. The lattice distance on the surface and the layer-by-layer distance are 0.95 and 1.8 μm, respectively. Compared with the simulated interference pattern shown in the inset image, the lattice was shrunk in the vertical direction of the film by 25% due to a pinning effect (12).

The activation of the SU-8 surface with the Pd catalyst was achieved by dipping the SU-8 woodpile structure in the catalyst solution of $[PdCl_4]^{2-}$ ions. Meanwhile, the native surface of SU-8 was negatively charged due to hydroxyl groups generated by a cross-linking reaction of the epoxy groups. Since the isoelectric point of hydroxide ions on the SU-8 was reported to be between pH 2 and 4 and the pH of the catalyst solution was about 2.5, the cross-linked SU-8 surface has a very weak positive charge in this catalyst solution (13). Hence, there might be a weak electrostatic attraction that would attach palladium ions, $[PdCl_4]^{2-}$ onto the surface. The elemental analysis by EDX showed that no Pd was deposited on the SU-8 surface (Table 1).

The surface of the SU-8 was treated with a positively charged polyelectrolyte to attract catalyst anions, and alternating coatings of positively and negatively charged polyelectrolytes (PAH and PAA) were applied to control the amount of catalyst deposited. In the case of PAH and PAA multilayers, it is known that surface compositions can be determined by the pH of the polyelectrolyte solutions (14). PAH solution at pH 7.5 and PAA solution at pH 3.5 were

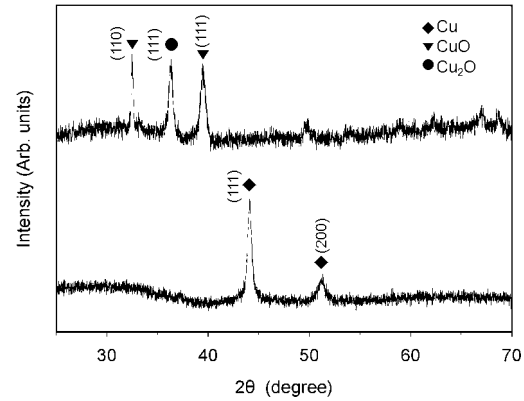

FIGURE 2. X-ray diffraction patterns of copper by electroless deposition and oxidized copper at 400 °C in air.

used; under these conditions, it is known that the surface is dominated by the last polyelectrolyte coating applied (14). In our experiment, after the first coating of PAH on bare SU-8, a catalytic solution containing $[PdCl_4]^{2-}$ ions was applied and subsequently the PAA coating was applied. The amount of catalyst can be controlled by the number of coatings, and in this experiment, this step for applying both coatings was repeated four times. Since the pK_a of the allylamine groups in PAH is around 7, PAH has a positive charge in acid catalyst solution. The PAH surface might adsorb $[PdCl_4]^{2-}$ ions effectively by electrostatic attraction. The other advantage of the coating of PAA and PAH is that the reduction of Pd ions into metallic Pd can be achieved simultaneously by ligand exchange with ionized carboxylates on the PAA (14). EDX analysis clearly showed that metallic Pd was found on the surface of the multilayer polyelectrolyte treated SU-8 surface (Table 1).

Copper electroless deposition was applied to coat the activated surface of the SU-8 woodpile structure with copper. Electroless copper was deposited autocatalytically from an alkaline solution of copper complex containing formaldehyde as the reducing agent. Previously, electrodeposition was used to successfully deposit cuprous oxide into 3D patterned structures (1). Compared with the electrodeposition approach, the electroless method is simpler as it does not require patterns on a conducting substrate or an applied external voltage. The growth rate of the conformal shell can also be changed in a controlled manner by altering, for example, the deposition time, the temperature or the reducing agent. For our deposition onto the woodpile structure, the growth rate of copper was about 50 nm/min. We determined that the copper was uniformly coated through the 3D SU-8 structures as shown in Figure S1 in the Supporting Information. XRD measurements showed that the copper grown by electroless deposition preferred the Cu(111) orientation over Cu(200) (Figure 2), as would be expected for growth at a high pH (15).

Calcination at 400 °C in air was then performed to remove the polymeric woodpile template and simultaneously oxidize the copper into copper oxide. Images c and d in Figure 1 show SEM images of the inverted woodpile copper oxide. The lattice distance on the surface and layer-by-layer distance are 0.9 and 1.1 μm, respectively. Copper

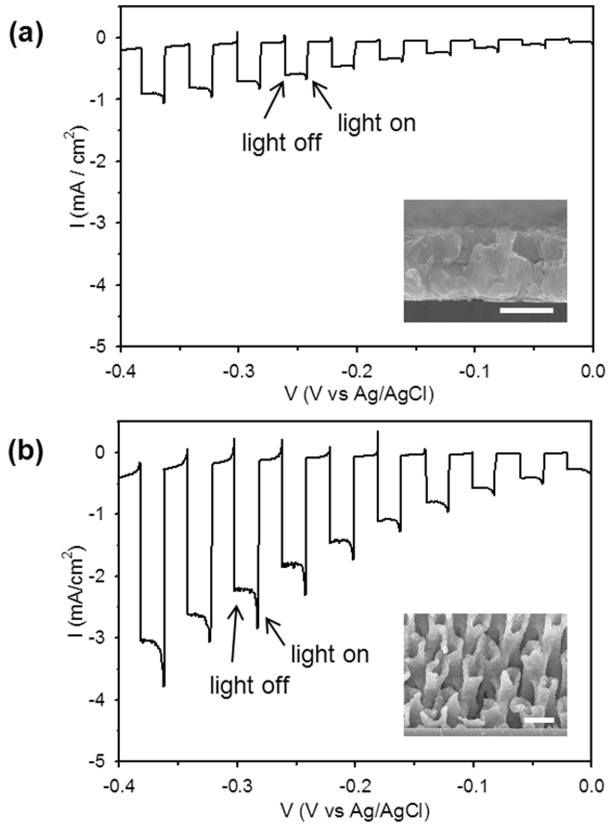

FIGURE 3. Photocurrent−voltage responses of (a) bare copper oxide and (b) 3D woodpile copper oxide structures. (Scale bar, 1 μm.)

can have two oxidation states: cuprous oxide (Cu_2O) and cupric oxide (CuO). The composition and crystalline phase of oxidized copper can be changed by varying the growth or the oxidizing conditions, such as temperature or the environment (17). In general, the formation of cupric oxide is favored during high temperature treatment because it is thermodynamically stable. As shown in Figure 2, XRD was measured to investigate the crystalline composition of oxidized copper. The peak assignments obtained using peak analysis software (Crystalimpact Inc.) indicated that cuprous oxide and cupric oxide coexist in the copper oxide woodpile structure.

The photocurrent response was measured under illumination. It is known that the photocurrent of copper oxide is induced by the creation of electron−hole pairs and the subsequent increase of minority carriers of electrons for p-type semiconductors under illumination (18). Photogenerated electrons transferred onto the copper surface reduce oxygen into hydrogen peroxide. Here, the chopped laser light (~3 W/cm^2) was periodically illuminated on the sample at a rate of 1 s exposure following every 1 s unilluminated, and the current was recorded while the voltage was changed from 0 to −0.4 V. We compared the photocurrent response of the 3D woodpile porous electrode structure of copper oxide and a film prepared by the same deposition procedure without the SU-8 structure. For both samples, a clear increase in the magnitude of the cathodic photocurrent was seen under laser exposure, as shown in Figure 3. The photocurrent was reduced when oxygen was not bubbled through the electrolyte solution or after several scans (not

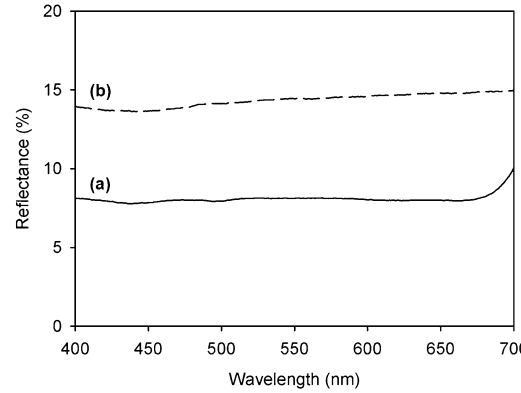

FIGURE 4. Diffuse reflectance spectra of (a) flat and (b) 3D woodpile copper oxide films.

shown). These findings demonstrate the absorption of the visible light by copper oxide and subsequent photoelectroreduction of oxygen on the surface. Meanwhile, it is noteworthy that the maximum photocurrent for flat film and 3D woodpile porous electrodes in the range −0.35 and −0.40 V is −1 and −3 mA/cm^2, respectively. Thus, 3D porous copper oxide electrodes show an increase of a factor of 3 in the cathode photocurrent when exposed to light. It has been reported that as the electrode becomes thicker, the photocurrent increases because of an increase in photon absorption (19). We compared the effective thickness of the flat film and 3D structures of copper oxide. The thickness of the flat copper oxide film was 1.5 μm. The effective thickness of the 3D copper oxide film was estimated to be ~1.0 μm, considering the thickness of the 3D copper oxide structures (4.7 μm) and the estimated filling fraction of 20% of copper oxide in 3D structures obtained from surface SEM images. Thus, the large photocurrent for 3D copper oxide structures might be mainly attributed to the fact that the increase in the surface area reduces the distance to the copper oxide surface and thus the charge transport length, hence reducing the rate of recombination of charge carriers.

Meanwhile, we measured diffuse reflectance spectra of flat and 3D porous copper oxide films. In our experiment, photonic bandgap properties of 3D woodpile structures cannot play any role: the photonic bandgap in the direction perpendicular to the film was estimated to be within infrared region by Bragg's law, which is outside the wavelength region of the exposed laser (20). Figure 4 shows that the reflectance of the 3D copper oxide films was twice that of the flat film on average in the visible-light range. Thus, the higher scattering of 3D woodpile porous structures can enhance the absorption of light (488 nm wavelength), resulting in additional enhancement of the photocurrent.

In summary, we used 3D holographic lithography to produce 3D porous copper oxide for use as photoelectrochemical electrodes. Multibeam interference patterning via a multifaceted prism produced a 3D woodpile SU-8 structure. The layer-by-layer coating with polyelectrolytes allowed facile modification of SU-8 structures and activation of the surface with catalysts. Electroless deposition of copper and subsequent calcination removed the SU-8 templates and simultaneously produced copper oxide. The 3D copper oxide

electrode showed an enhanced electrochemical response under exposure to visible laser light. This photoelectrochemical response revealed that a high surface area of 3D copper oxide structure was favored in electrode applications. We believe this type of electrode fabricated from holographically defined templates allows control of the morphology (e.g., pore size and network) over a wide range with high fidelity. Moreover, the uniform pore size throughout the pore network and the triply connected pore network allow easy infiltration of electrolytes and high mechanical strength, which is an advantage for use as electrodes for solar energy harvesting and storage.

Acknowledgment. This work was supported by the National Research Foundation of Korea (NRF-2010-C1AAA001-2010-0028958, NRF-2010-0011024). The Korea Basic Science Institute is also acknowledged for the scanning electron microscope measurements.

Supporting Information Available: Additional SEM image (PDF). This material is available free of charge via the Internet at http://pubs.acs.org.

REFERENCES AND NOTES

(1) Miyake, M.; Chen, Y. C.; Braun, P. V.; Wiltzius, P. *Adv. Mater.* **2009**, *21*, 3012.
(2) Zhang, X. J.; Wang, G. F.; Wu, H. B.; Zhang, D.; Zhang, X. Q.; Li, P.; Wu, H. Q. *Mater. Lett.* **2008**, *62*, 4363.
(3) Xiang, J. Y.; Tu, J. P.; Huang, X. H.; Yang, Y. Z. *J. Solid State Electrochem.* **2008**, *12*, 941.
(4) Chauhan, D.; Satsangi, V. R.; Dass, S.; Shrivastav, R. *Bull. Mater. Sci.* **2006**, *29*, 709.
(5) Chaudhary, Y. S.; Agrawal, A.; Shrivastav, R.; Satsangi, V. R.; Dass, S. *Int. J. Hydrogen Energy* **2004**, *29*, 131.
(6) Li, J.; Shi, Y.; Cai, Q.; Sun, Q. Y.; Li, H. D.; Chen, X. H.; Wang, X. P.; Yan, Y. J.; Vrieling, E. G. *Cryst. Growth Des.* **2008**, *8*, 2652.
(7) Sahoo, S.; Husale, S.; Colwill, B.; Lu, T. M.; Nayak, S.; Ajayan, P. M. *ACS Nano* **2009**, *3*, 3935.
(8) Li, X.; Tao, F. F.; Jiang, Y.; Xu, Z. *J. Colloid Interface Sci.* **2007**, *308*, 460.
(9) Moon, J. H.; Yang, S. *Chem. Rev.* **2010**, *110*, 547.
(10) Tam, W. Y. *J. Opt. Soc. A* **2007**, *9*, 1076.
(11) Pang, Y. K.; Lee, J. C. W.; Ho, C. T.; Tam, W. Y. *Opt. Express* **2006**, *14*, 9113.
(12) Zhu, X. L.; Xu, Y. G.; Yang, S. *Opt. Express* **2007**, *15*, 16546.
(13) Sikanen, T.; Heikkila, L.; Tuornikoski, S.; Ketola, R. A.; Kostiainen, R.; Franssila, S.; Kotiaho, T. *Anal. Chem.* **2007**, *79*, 6255.
(14) Wang, T. C.; Chen, B.; Rubner, M. F.; Cohen, R. E. *Langmuir* **2001**, *17*, 6610.
(15) Kim, Y. S.; Bae, D. L.; Yang, H. C.; Shin, H. S.; Wang, G. W.; Senkevich, J. J.; Lu, T. M. *J. Electrochem. Soc.* **2005**, *152*, C89.
(16) Byeon, J. H.; Lee, R. H.; Hwang, J. *J. Phys. D: Appl. Phys.* **2009**, 42.
(17) Brown, K. E. R.; Choi, K. S. *Chem. Commun.* **2006**, 3311.
(18) de Jongh, P. E.; Vanmaekelbergh, D.; Kelly, J. J. *J. Electrochem. Soc.* **2000**, *147*, 486.
(19) Chaudhary, Y. S.; Agrawal, A.; Shrivastav, R.; Satsangi, V. R.; Dass, S. *Int. J. Hydrogen Energy* **2003**, *29*, 131.
(20) The photonic bandgap in this direction can be estimated by Bragg's law to be 5.6 μm using the estimated filling fraction of 0.3 and refractive index of 2.4 for copper oxide.

AM100773H